

Supporting Information to be published electronically

Solution Speciation, Kinetics, and Observing Reaction Intermediates in the Alkylation of Oxidovanadium Compounds

*Jessica M. Fautch and Jonathan J. Wilker**

Department of Chemistry, Purdue University
560 Oval Dr., West Lafayette, IN 47907-2084

Inorg. Chem.

- Figure S1.** Concentration-versus-time kinetic plot for the 10:1 reaction of K[VO₂(salhyph(H)₂)].CH₃OH and (CH₃CH₂O)₂SO₂
- Figure S2.** ⁵¹V NMR spectra of a 1:1 reaction between (CH₃CH₂O)₂SO₂ and K[VO₂(salhyph(H)₂)].CH₃OH in progress and in DMSO-*d*₆
- Figure S3.** ⁵¹V NMR spectra in acetone-*d*₆ of synthesized vanadium compounds
- Figure S4.** ⁵¹V NMR spectra in DMSO-*d*₆ of synthesized vanadium compounds
- Figure S5.** ¹H NMR spectra of a 1:1 reaction between (CH₃CH₂O)₂SO₂ and K[VO₂(salhyph(H)₂)].CH₃OH in progress and in DMSO-*d*₆. Also ¹H NMR spectra in DMSO-*d*₆ of synthesized vanadium compounds
- Figure S6.** ¹H NMR spectra of a 1:1 reactions between (CH₃CH₂O)₂SO₂ and K[VO₂(salhyph(H)₂)].CH₃OH in progress and in acetone-*d*₆. ¹H NMR spectra in acetone-*d*₆ of synthesized vanadium compounds
- Figure S7.** ¹H and ⁵¹V NMR spectra in DMSO-*d*₆ of synthesized {[VO(salhyph(H)₂)]₂O}
- Section S8.** Attempts to determine the rate law and reaction order
- Figure S8.** Plot of *k*_{obs} values vs. V⁻_{free} concentrations. Data from KPF₆ addition experiments and variation of K[VO₂(salhyph(H)₂)].CH₃OH concentrations.

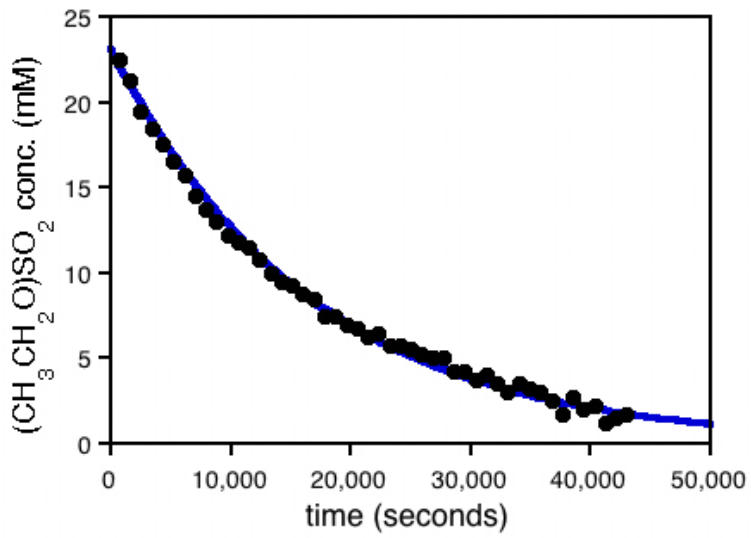


Figure S1. Plot of $(\text{CH}_3\text{CH}_2\text{O})_2\text{SO}_2$ concentrations-versus-time for the 10:1 (200:20 mM) reaction of $\text{K}[\text{VO}_2(\text{salhyph}(\text{H})_2)] \cdot \text{CH}_3\text{OH}$ and $(\text{CH}_3\text{CH}_2\text{O})_2\text{SO}_2$. Concentration data were obtained by integrating the methylene ^1H NMR peaks of $(\text{CH}_3\text{CH}_2\text{O})_2\text{SO}_2$.

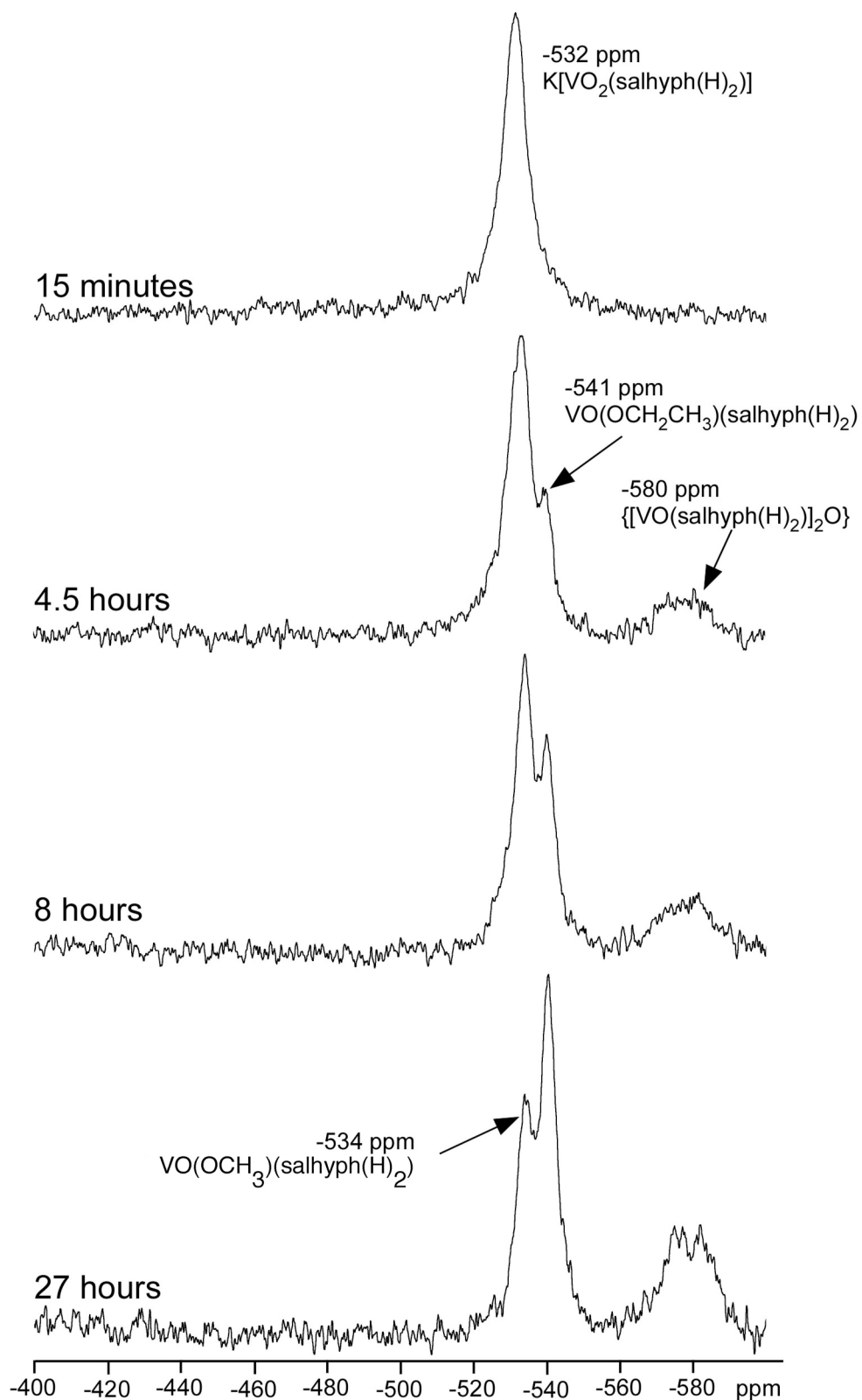


Figure S2. The ^{51}V NMR spectra taken at varied times for a 1:1 alkylation reaction between $\text{K}[\text{VO}_2(\text{salhyph(H)}_2)] \cdot \text{CH}_3\text{OH}$ and $(\text{CH}_3\text{CH}_2\text{O})_2\text{SO}_2$ (50 mM each) in $\text{DMSO}-d_6$.

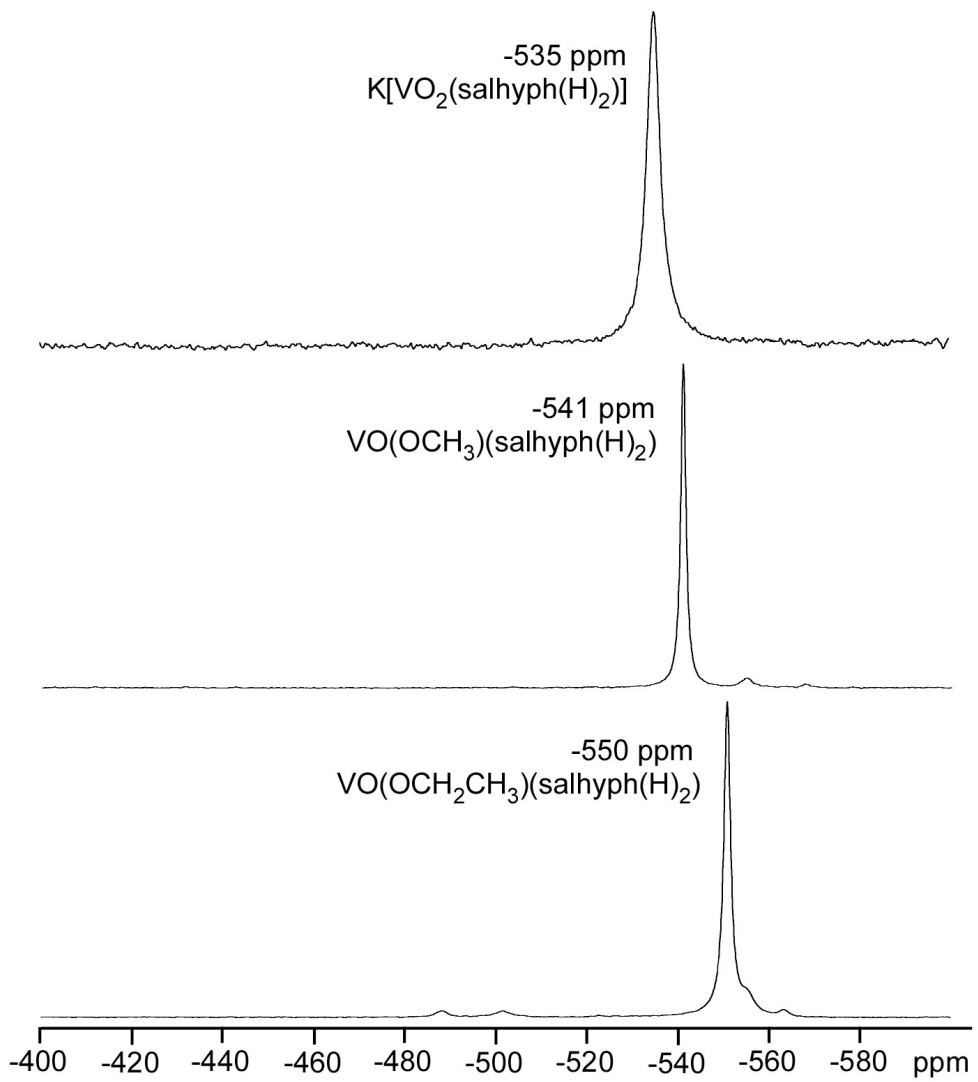


Figure S3. ^{51}V NMR spectra of three synthesized compounds in acetone- d_6 . The top spectrum shows $\text{K}[\text{VO}_2(\text{salhyph(H)}_2)] \cdot \text{CH}_3\text{OH}$ at -535 ppm. The middle spectrum is $\text{VO}(\text{OCH}_3)(\text{salhyph(H)}_2)$ at -541 ppm and the bottom spectrum is $\text{VO}(\text{OCH}_2\text{CH}_3)(\text{salhyph(H)}_2)$ at -550 ppm.

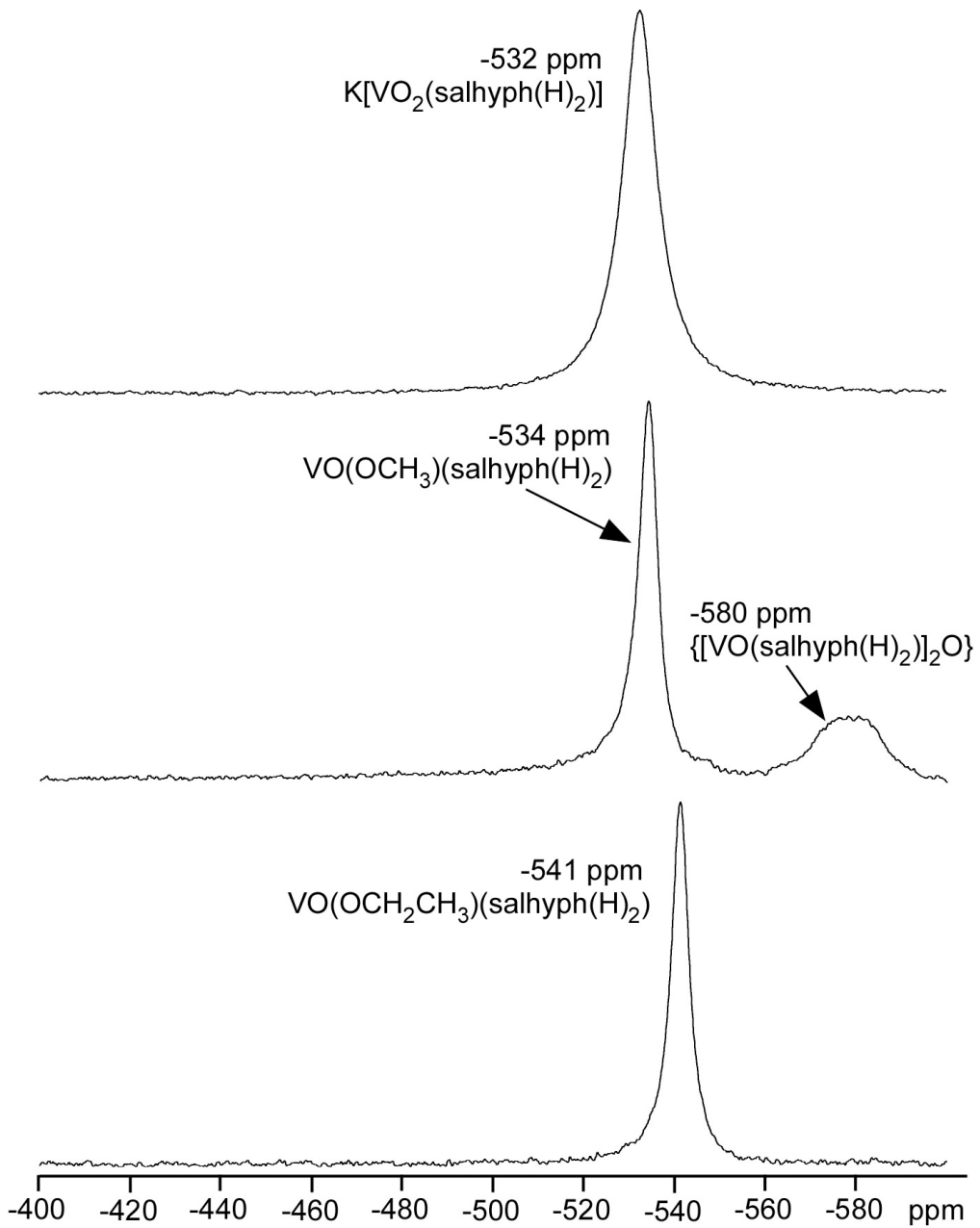


Figure S4. ^{51}V NMR spectra of three synthesized compounds in $\text{DMSO}-d_6$. The top spectrum shows $\text{K}[\text{VO}_2(\text{salhyph(H)}_2)] \cdot \text{CH}_3\text{OH}$ at -532 ppm . The middle spectrum is $\text{VO(OCH}_3\text{)(salhyph(H)}_2)$ at -534 ppm and the bottom spectrum is $\text{VO(OCH}_2\text{CH}_3\text{)(salhyph(H)}_2)$ at -541 ppm .

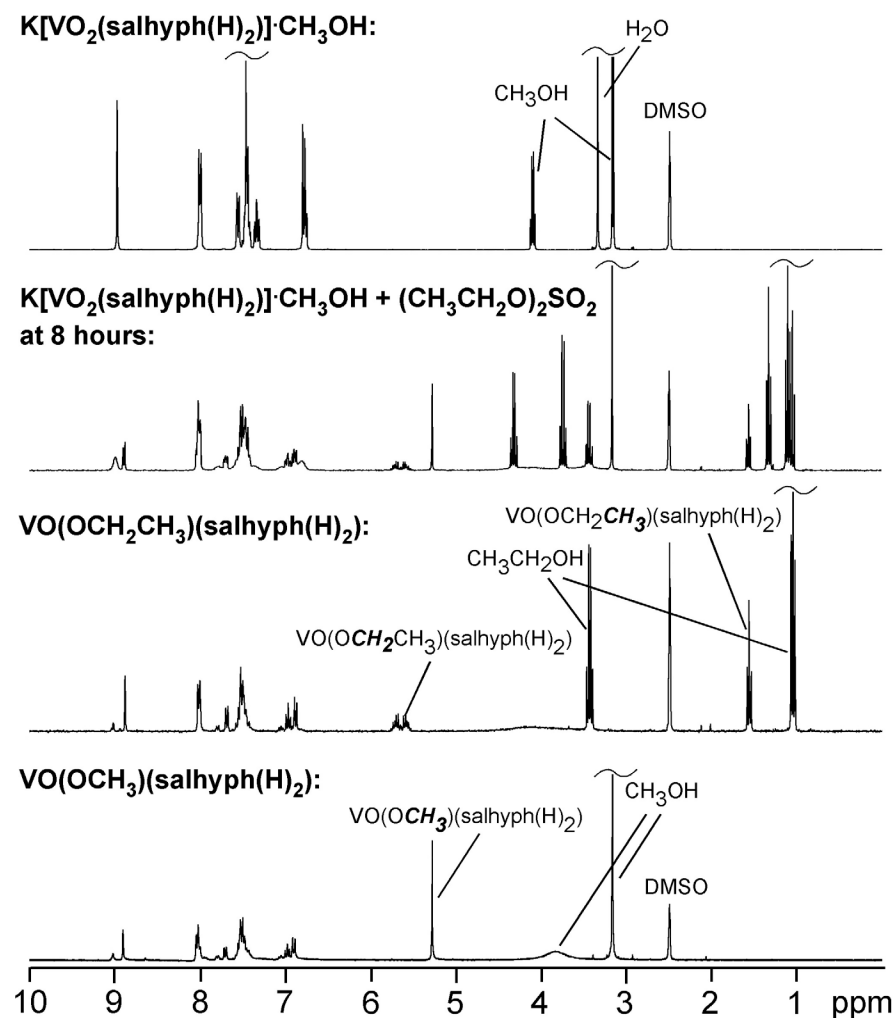


Figure S5. ^1H NMR spectra of three synthesized compounds and one alkylation reaction in $\text{DMSO}-d_6$. The top spectrum shows $\text{K}[\text{VO}_2(\text{salhyph(H)}_2)] \cdot \text{CH}_3\text{OH}$. The next spectrum is an alkylation reaction in progress. The following spectrum is $\text{VO}(\text{OCH}_2\text{CH}_3)(\text{salhyph(H)}_2)$. The bottom spectrum is $\text{VO}(\text{OCH}_3)(\text{salhyph(H)}_2)$.

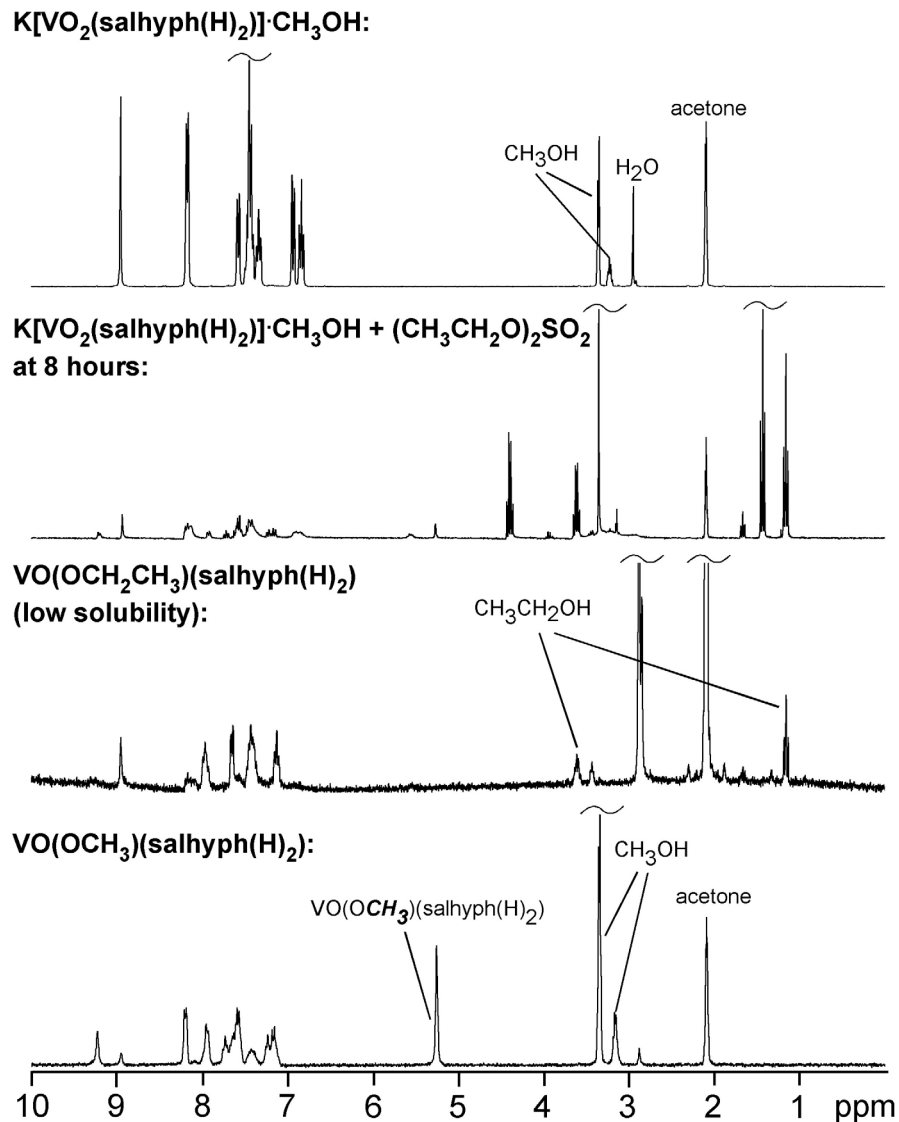


Figure S6. ^1H NMR spectra of three synthesized compounds and one alkylation reaction in acetone- d_6 . The top spectrum shows $\text{K}[\text{VO}_2(\text{salhyph}(\text{H})_2)] \cdot \text{CH}_3\text{OH}$. The next spectrum is an alkylation reaction in progress. The following spectrum is $\text{VO}(\text{OCH}_2\text{CH}_3)(\text{salhyph}(\text{H})_2)$. The bottom spectrum is $\text{VO}(\text{OCH}_3)(\text{salhyph}(\text{H})_2)$.

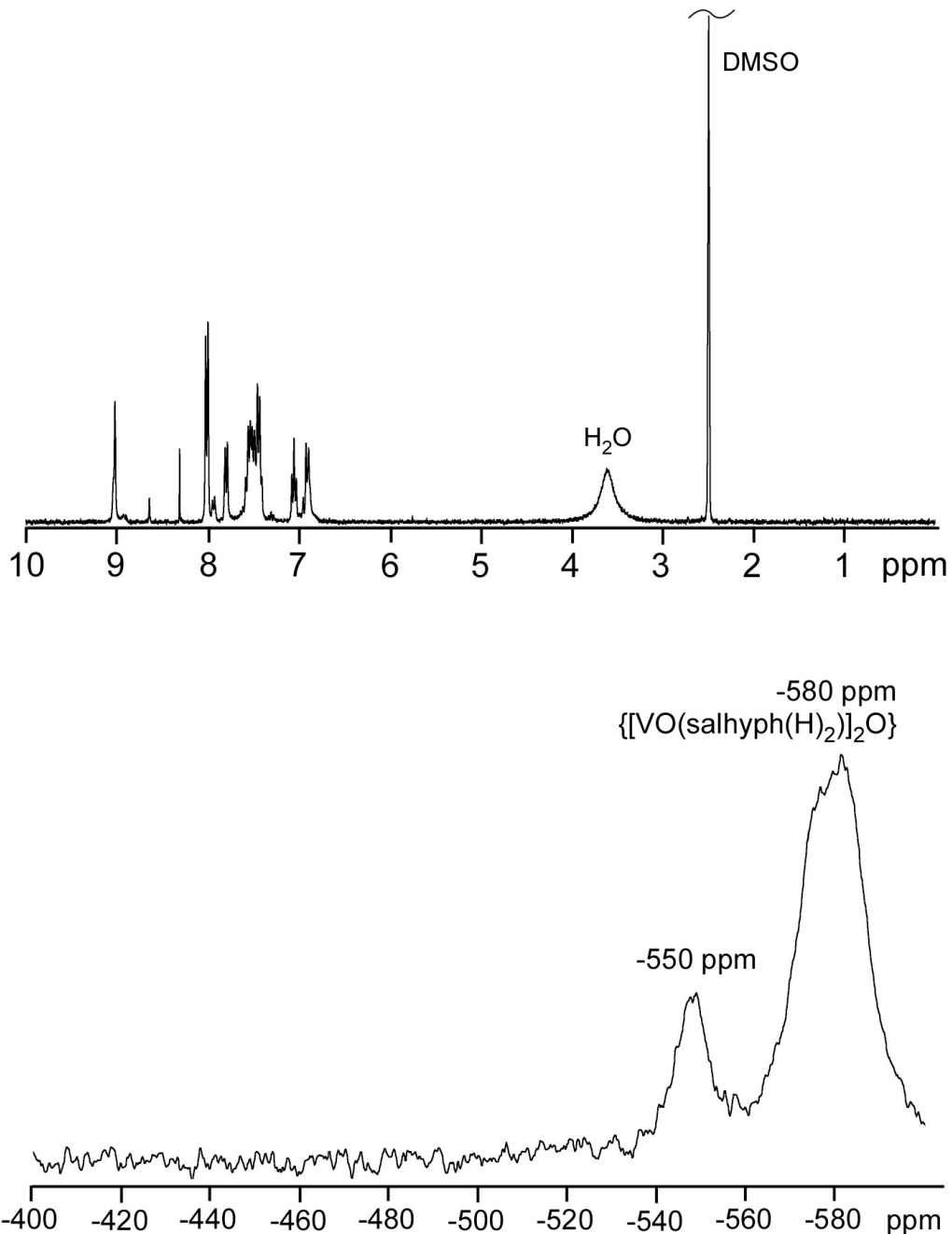


Figure S7. Top: ^1H NMR spectrum of the synthesized, crystalline $\{[\text{VO}(\text{salhyph}(\text{H})_2)]_2\text{O}\}$ compound in $\text{DMSO}-d_6$. Bottom: The ^{51}V NMR spectrum of the same dinuclear compound in $\text{DMSO}-d_6$.

Section S8.

Attempts to determine the rate law and reaction order

The reaction rate law was investigated. Recall it was noted that there appeared to be no dependence of alkylation rate constants upon vanadium concentrations, in Figure 2. However, it is known that ion-pairing is a significant component of this system and decreases the amount of V^-_{free} available to react with $(\text{CH}_3\text{CH}_2\text{O})_2\text{SO}_2$ (c.f., Scheme 1). One should examine the alkylation reactions in terms of $[V^-_{\text{free}}]$ rather than $[V^-_{\text{total}}]$. Determining the reaction order with respect to vanadium requires varying $[V^-_{\text{free}}]$ to examine potential influences upon k_{obs} values. At this point there are two sets of data to explore in which $[V^-_{\text{free}}]$ was varied. In the first experiment, the V^-_{total} concentrations were altered (Figure 2). Second, $[V^-_{\text{total}}]$ was held constant and different amounts of KPF_6 were added. Both experiments can provide rate constants as a function of different V^-_{free} concentrations.

First we examine data from the experiment in which the amount of K^+ in solution was changed by using added KPF_6 . This added KPF_6 will decrease the available, reactive $[V^-_{\text{free}}]$. Note that KPF_6 , itself, can exhibit ion-pairing as well. The smaller K^+ cation may form a tighter ion-pair than the $(n\text{-C}_4\text{H}_9)_4\text{NPF}_6$ conductivity standard (Figure 3B). Thus all added KPF_6 cannot be treated as a simple K^+ source. Ion-pairing of KPF_6 will diminish the effect of added K^+ upon the ion-pairing of $\text{K}^+ + V^-_{\text{free}} \rightleftharpoons \text{KV}$.

With five coexisting species in solution, K^+ , V^- , PF_6^- , KV , and KPF_6 , determining the concentration of V^-_{free} can become complex. A good place to start is to examine the data with no added KPF_6 and starting KV (or V^-_{total}) at 200 mM. This alkylation reaction yields a pseudo-first-order rate constant of $k_{\text{obs}} = 5.3 \times 10^{-5} \text{ s}^{-1}$ (Table 1). Adding KPF_6 and

keeping KV concentration constant at 200 mM will push $\text{K}^+ + \text{V}^-$ more toward the less reactive KV. Consequently lower k_{obs} values are to be anticipated. If it is assumed that all added KPF_6 behaves as K^+_{free} , the standard equation of ion-pairing shown above (Equation 1) is used, and the concentration of V^-_{free} is determined, addition of 125 mM KPF_6 is expected to drop the rate constant from $k_{\text{obs}} = 5.3 \times 10^{-5} \text{ s}^{-1}$ to $k_{\text{obs}} = 2.1 \times 10^{-5} \text{ s}^{-1}$. With addition of 250, 375, or 500 mM KPF_6 , the observed rate constants may be expected to drop to 1.3×10^{-5} , 9.7×10^{-6} , and $7.6 \times 10^{-6} \text{ s}^{-1}$, respectively. Seen in Figure 4 are the measured rate constants. The predicted rate constants are all lower than those actually observed. A likely explanation for this discrepancy is ion-pairing of the added KPF_6 at the high concentrations used here. This KPF_6 ion-pairing yields decreased available K^+_{free} for ion-pairing with V^-_{free} , thereby providing less rate suppression. The differences in observed versus predicted rate constants can be used to determine the actual concentration of V^-_{free} . A ratio between the predicted k_{obs} value and the measured k_{obs} is multiplied by the concentration of V^-_{free} at 0 mM KPF_6 (60.4 mM) to provide the $[\text{V}^-_{\text{free}}]$ in each case of added KPF_6 (125, 250, 375, and 500 mM). With added KPF_6 at 125 mM, the V^-_{free} concentration is 44.0 mM. Similarly, at 250, 375, and 500 mM added KPF_6 the concentrations of V^-_{free} are 41.6, 33.4, and 36.7 mM, respectively. These $[\text{V}^-_{\text{free}}]$ points can then be placed on a k_{obs} vs. $[\text{V}^-_{\text{free}}]$ plot. Data from this experiment are noted with filled squares in the plot of Figure S8.

Next we examine the k_{obs} vs. $[\text{V}^-_{\text{total}}]$ data from the earlier experiments in which KPF_6 was kept at 0 mM and the total vanadium in solution was varied, seen in Figure 2. With the ion-pairing equilibrium constant of $K_{\text{IP}} = 0.041 \text{ M}^{-1}$, one can now determine the amount of anionic V^-_{free} in each of these solutions. With a starting

$\text{K}[\text{VO}_2(\text{salhyph}(\text{H})_2)] \cdot \text{CH}_3\text{OH}$ concentration of 100 mM, approximately 39 mM of the compound exists as the reactive, free V^- anion. Likewise, at starting $\text{K}[\text{VO}_2(\text{salhyph}(\text{H})_2)] \cdot \text{CH}_3\text{OH}$ concentrations of 300, 400, and 500 mM the V^-_{free} concentrations are 72, 77, and 90 mM, respectively. After correlating the observed rate constants to each V^-_{free} concentration, we can add these points to the V^-_{free} versus k_{obs} plot of Figure S8. These data are plotted with filled circles . The background/control reaction, described earlier (e.g., see Figure 1), has a rate constant of $1.1 \times 10^{-5} \text{ s}^{-1}$ and is also shown with a closed circle on the $[\text{V}^-_{\text{free}}] = 0$ y-axis (Figure S8).

If this $[\text{V}^-_{\text{free}}]$ versus k_{obs} plot shows a straight line with positive slope and a y-intercept at the background reaction, it could be concluded that there is a first-order dependence of the reaction upon $[\text{V}^-_{\text{free}}]$. Note that the line is not expected to intercept the origin where $[\text{V}^-_{\text{free}}] = 0$. Looking at Figure S8, unfortunately, the data do not provide a clear correlation. Several factors might contribute to noise in data. With each kinetic run taking place over the course of 12 hours, there is a chance for drift in the NMR spectrometer. Continuous clean kinetic data on time scales over 12 hours could not be obtained, owing to limitations from instrument access and costs. Attempts to obtain spectra beyond 12 hours involved removing the sample and returning to the instrument periodically. The resulting time-versus-concentration plots were quite noisy. Generally speaking, NMR integrals may not be the source of the cleanest kinetic data compared to, say, UV-vis spectroscopy. In order to study these reactions at the concentrations described, however, NMR spectroscopy proved to be the most suitable. Further errors may result from the calculations of $[\text{V}^-_{\text{free}}]$ for each data point. Attempting to syringe the

very small quantities of $(CH_3CH_2O)_2SO_2$ (2.6 μL) and DMF (7.4 μL) could also contribute to scatter in the data.

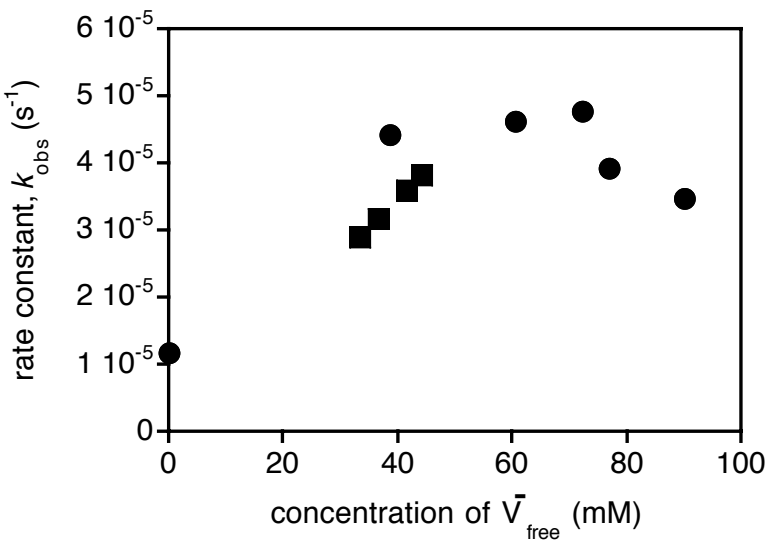


Figure S8. Plot of k_{obs} values versus $\text{V}^{\cdot}_{\text{free}}$ concentration. Squares indicate data from the KPF_6 addition experiments with $\text{K}[\text{VO}_2(\text{salhyph(H)}_2)] \cdot \text{CH}_3\text{OH}$ at 200 mM. Circles show data from variation of $\text{K}[\text{VO}_2(\text{salhyph(H)}_2)] \cdot \text{CH}_3\text{OH}$ concentrations. The background reaction with no vanadium or KPF_6 is also shown as a circle, on the y-axis.